

Analysis of Monte Carlo methods applied to blackbody and lower emissivity cavities

Robert J. Pahl and Mark A. Shannon

Monte Carlo methods are often applied to the calculation of the apparent emissivities of blackbody cavities. However, for cavities with complex as well as some commonly encountered geometries, the emission Monte Carlo method experiences problems of convergence. The emission and absorption Monte Carlo methods are compared on the basis of ease of implementation and convergence speed when applied to blackbody sources. A new method to determine solution convergence compatible with both methods is developed, and the convergence speeds of the two methods are compared through the application of both methods to a right-circular cylinder cavity. It is shown that the absorption method converges faster and is easier to implement than the emission method when applied to most blackbody and lower emissivity cavities. © 2002 Optical Society of America

OCIS codes: 000.4430, 120.4570, 230.6080, 300.2140.

1. Introduction

Blackbody cavities have an important role as calibration sources in such fields as radiometry, pyrometry, and spectroscopy. Analysis of the emission characteristics of experimental blackbodies is needed to reach more accurate results in these fields. Analytical results giving the apparent (effective) emissivities of blackbody cavities generally become intractable when nonaxisymmetric cavities or cavities with nonisothermal and specular cavity wall properties are analyzed. Monte Carlo numerical techniques therefore have been used extensively in blackbody cavity analysis for cases in which the geometries are more complicated and nonisothermal and specular material cavity wall properties are present.

In the literature, two distinct methods have been presented for use of the Monte Carlo technique to determine the apparent emissivity of blackbody cavities. Both methods are derived from radiant energy transfer theory and have been used to measure the apparent emissivity of several basic cavity designs.

The first Monte Carlo method developed for cavity

analysis is the emission method, which is based on an energy balance at each emitting surface. This method has been used to examine cavity geometries such as the cylinder¹ and right cone.² The results of these analysis match those of existing analytical results within the statistical error of the Monte Carlo method. Improvements to this technique have been developed to increase convergence³ and to model surfaces with more realistic radiative properties.⁴

The second method that was developed is the absorption method, which is based on the integral equations arising from radiative energy transfer analysis. This method has also been used to examine various cavity geometries,⁵⁻⁷ which were then compared with existing analytical results. This method has been improved⁸⁻¹⁰ by techniques similar to those used to improve the emission method.

Both emission and absorption Monte Carlo methods can be used in the analysis of blackbody cavities. A direct comparison of these two methods is needed to determine which method is preferred in terms of speed of convergence and ease of implementation in different applications. It is our goal in this paper to provide such a general comparative analysis of the emission and absorption Monte Carlo methods as applied to cavities. In this analysis, we show that, in the general case, the absorption method has a greater ease of implementation. We also show that, as a cavity is made to have more surfaces with high emissivity that do not directly face the cavity aperture or face the aperture at oblique angles, the emission method will lose its speed of convergence, whereas

The authors are with the University of Illinois, Urbana-Champaign, Urbana, Illinois 61801-2906. M. Shannon's e-mail address is mas1@uiuc.edu.

Received 1 June 2001; revised manuscript received 9 October 2001.

0003-6935/02/040691-09\$15.00/0

© 2002 Optical Society of America

the absorption method will experience a minimal loss in its speed of convergence.

In this paper we obtain the above objectives by comparing both methods in terms of implementation and convergence speed. To quantify the difference in convergence speed, new convergence criteria are developed that are compatible with both methods. These convergence criteria are then used in the application of both methods to a cylindrical blackbody source, which will quantify the difference in convergence speed between the two methods as the cavity geometry is modified to have more surfaces that face the aperture at oblique angles. Finally, the results of the comparison of the emission and absorption Monte Carlo methods are summarized.

2. Theory

A. Background

The Monte Carlo emission and absorption methods both have their origins in radiant energy transfer. The emission method is based on an energy balance at each surface, and the absorption method is based on the integral series solution for surface reflectivity. For both methods, only an outline of the theoretical development is given, and the cavity wall surfaces are assumed to be isothermal, gray, and diffuse.

The theoretical basis for the emission method of Monte Carlo cavity analysis is in the form of an energy balance. Each surface emits energy bundles having energy

$$E_{\text{bun}} = \frac{\epsilon_w \sigma T_w^4 A_w}{N}, \quad (1)$$

where T_w is the temperature of the emitting surface, A_w is the total surface area of the cavity walls, ϵ_w is the surface emissivity, σ is the Stefan-Boltzmann constant, and N is the total number of energy bundles emitted by all cavity surfaces. The initial location of bundle emission and the direction of the bundle are determined by probability functions. These bundles are then traced to their next surface intersection where either absorption or reflection takes place as determined by the probability function of the material properties of that surface. The calculated net energy flux at a given surface is thus determined when we take the difference between the number of bundles absorbed and the number of bundles emitted by that surface. We thus find the hemispherical apparent emissivity of the aperture by dividing the net flux of the aperture E_{ap} by the flux of a perfectly emitting surface σT_w^4 , or

$$\epsilon_{\text{app}} = \frac{E_{\text{ap}}}{\sigma T_w^4 A_{\text{ap}}} = \frac{N_{\text{out}} E_{\text{bun}}}{\sigma T_w^4 A_{\text{ap}}} = \frac{N_{\text{out}}/A_{\text{ap}}}{N/A_w} \epsilon_w, \quad (2)$$

where N_{out} is the number of bundles that exit through the aperture and A_{ap} is the surface area of the aperture.

The derivation of the absorption Monte Carlo method arises from the integral equation for the ap-

parent emissivity at the aperture of a cavity. The apparent directional reflectivity of a cavity aperture is given by the series solution

$$\rho_{\text{app}}'(X) = f_1 \rho_w + f_2 \rho_w^2 + f_3 \rho_w^3 + \dots, \quad (3)$$

where ρ_w is the reflectivity of the cavity wall surfaces and X is the location of an elemental area of the cavity surface. We can find the apparent total hemispherical reflectivity ρ_{app} by integrating the apparent directional reflectivity from Eq. (3) over all directions, over the cavity walls, and over the surface area of the aperture.

The coefficients of Eq. (3), f_i , are purely geometric in nature and are given by¹¹

$$\begin{aligned} f_1 &= \int_{\text{app}} dF(X, A), \\ f_2 &= \int_{\text{app}} dF(X, A) \int_{X_1} dF(X, X_1), \\ f_3 &= \int_{\text{app}} dF(X, A) \int_{X_1} \int_{X_2} dF(X, X_2) dF(X_2, X_1), \\ &\vdots \\ f_i &= \int_{\text{app}} dF(X, A) \int_{X_1} \int_{X_2} \dots \int_{X_i} dF(X, X_i) \dots dF \\ &\quad \times (X_3, X_2) dF(X_2, X_1), \\ &\vdots, \end{aligned} \quad (4)$$

where $dF(X_i, X_j)$ is the angle factor between surface elements dX_i and dX_j . These coefficients can be thought of as the fraction of energy leaving the cavity through the aperture after undergoing i reflections. In this manner, f_1 is the diffuse angle factor from a position on the cavity walls specified by X to the cavity aperture. For $i \geq 2$, these coefficients can become analytically intractable for even simple cone and cylinder geometries; therefore numerical techniques are used to calculate them.

The Monte Carlo technique can be used to determine these coefficients, as has been shown by Ono.⁵ A large number of energy bundles N originating from the cavity aperture surface are incident on the cavity walls. These bundles each carry an arbitrary, but identical, energy. On each impact, the subsequent direction for the energy bundle is determined by a probability distribution. The coefficients are then determined when we find the fraction of energy bundles N_i/N exiting after undergoing i reflections. The apparent total hemispherical reflectivity is found when we distribute the originating rays over the aperture surface and over 2π sr and take their sum, given by

$$\rho_{\text{app}} = \sum_{i=1}^{m^*} \frac{N_i}{N} \rho_w^i. \quad (5)$$

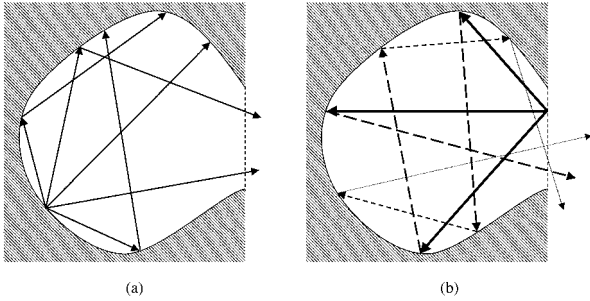


Fig. 1. Conceptual drawings of (a) the emission method and (b) the absorption method that show the principal differences between the two methods. In the emission method, the bundles are emitted from the cavity surfaces and are traced until absorbed by the cavity wall or exit the cavity. In the absorption method, the bundles are emitted from the aperture and are traced until they exit the aperture or until the reflection truncation limit m^* is reached.

In contrast to Eq. (3), Eq. (5) is the apparent reflectivity averaged over the whole aperture as opposed to that from a specific location on the cavity wall X . In addition, Eq. (5) is truncated at the m^* th reflection term where the value of ρ_w^i becomes negligible with respect to other terms of the sum. We estimated an upper limit to m^* for a given computer system round-off error Er by

$$m^* < \text{Int} \left(\frac{\log \text{Er}}{\log \rho_w} \right). \quad (6)$$

Another form of this series developed by Sapritsky and Prokhorov^{8,9} can be constructed when we separate out the bundles of each of the N_i terms of Eq. (5) and then sum all these bundles as individual terms, transforming that sum into the new form,

$$\rho_{\text{app}} = \frac{1}{N} \sum_{j=1}^N \rho_w^{m_j}, \quad (7)$$

where m_j is the number of reflections made by the j th bundle before exiting the cavity, limited by m^* . Using Kirchhoff's law, we then rewrite this sum in terms of the cavity's apparent total hemispherical emissivity as

$$\epsilon_{\text{app}} = \frac{\epsilon_w}{N} \sum_{j=1}^N \sum_{k=1}^{m_j} \rho_w^{k-1}. \quad (8)$$

Although both methods use the Monte Carlo technique, these two numerical methods differ on a number of key aspects. In the emission method, all cavity surfaces emit energy bundles, and the aperture itself only absorbs bundles as shown in Fig. 1(a). The bundles have a defined energy that is related to the surface area of the cavity. Upon each surface interaction, each bundle is either completely absorbed or completely reflected. Thus the Monte Carlo emission method is used to distribute energy between the cavity surfaces and the cavity aperture. In contrast, the absorption method uses an arbitrarily defined bundle energy, and bundles are emitted only by the aperture as shown in Fig. 1(b). Each

bundle is partially absorbed and is reduced in statistical weight by a factor of ρ_w at each surface interaction. In this way, the Monte Carlo absorption method is used to find the probability of energy returning to the aperture from the cavity surfaces.

B. Method Comparison

The differences between the emission and the absorption methods when applied to cavities can be brought forth when we look at three aspects of their use: distribution functions, rate of convergence, and applications. The first of these aspects, distribution functions related to the location of bundle emission, is now compared between the two Monte Carlo methods. In the emission method, each surface emits an identical number of bundles per surface area. Consequently, an overall distribution function is first found that weights each surface according to its fraction of the overall cavity surface. Then a probability distribution function is found for each i th surface in the j th coordinate direction so we can obtain a uniform distribution of emitted bundles across each surface. Assuming gray, isothermal cavity walls, these distribution functions are of the form

$$P_i(x_j) dx_j = \frac{1}{A} dA, \quad (9)$$

where x_j are coordinates of some cavity reference frame. Such functions are found for each coordinate and for each surface. Each of these probability functions is then integrated to find the cumulative distribution function,

$$R_{ij} = \int_0^{x_j} P_i(x_j') dx_j', \quad (10)$$

which is used to determine the position x_j on the i th surface by use of a random number R_{ij} between 0 and 1. If the geometry consists of a large number of small planar surfaces, this results in $i \times j$ integrals to be evaluated; for geometries consisting of nonplanar geometries, it can be a formidable task to solve Eq. (10).

In contrast to the emission method, the absorption method requires that only one distribution function be found over the aperture. Most experimental blackbody sources have a circular aperture residing in a single plane. Thus, for the absorption method, the calculation of distribution functions is independent of cavity geometry and therefore does not increase in complexity for cavities containing many planar or some nonplanar surfaces.

The second comparison to be made between the two methods deals with the speed of convergence of the algorithm. To compare the convergence speed of these two methods, a compatible convergence method for both methods is developed in Subsection 3.A. In this new convergence method, the output of the Monte Carlo algorithm is separated into separate, consecutive sets. The variance of these sets, in turn, is used to determine convergence. Any property or

effect that tends to increase this set variance will therefore increase the number of bundles required for convergence. Before we thoroughly develop this new convergence method, some general assertions can be made when we compare the convergence speed of the two Monte Carlo methods.

If one looks at the Monte Carlo emission equation, Eq. (2), one sees that the bundles are distributed on the cavity surface according to a bundle density:

$$\rho_B = \frac{N}{A_w}. \quad (11)$$

For a given number of bundles, the bundle density decreases as the surface area of the cavity increases. Although variance is, in general, dependent on the geometry and surface properties of the cavity in question, one expects the general behavior that, as the bundle density decreases, the variance of each set will increase. In turn, this leads to a larger number of emitted bundles required before the convergence criteria are met, which implies that, as cavity surface area A_w increases, the total number of bundles required for convergence must also increase. Also, in geometries with surfaces that face the cavity aperture at oblique angles, the contribution of such surfaces to the overall cavity apparent emissivity is small and subject to large variance because of multiple reflections. For a source containing such complex geometry, a large number of bundles is used to ensure a final result with low variance.

The number of bundles N is directly related to the speed of convergence in that, for each bundle, a computationally intensive ray-tracing subroutine, costing time τ , must be called a minimum of one time. The total computational time t for convergence can then be expressed as

$$t \cong N\bar{r}\tau, \quad (12)$$

where \bar{r} is the average number of reflections of a bundle before it exits the cavity or is absorbed by a cavity wall. In general, \bar{r} is dependent on both geometry and cavity wall material properties; however, for the emission method an upper bound on the average number of reflections per bundle can be found. If the aperture is replaced by an absorbing surface with radiative properties identical to the cavity walls, each bundle reflects until it is absorbed by a surface. At each surface interaction, the bundle has a probability of ρ_w of being reflected; therefore, for a constant ρ_w , the average number of reflections for the emission method is bounded by the power series

$$\bar{r}_{\text{emiss}} \leq \sum_{l=0}^{\infty} \rho_w^l = \frac{1}{1 - \rho_w}. \quad (13)$$

This upper bound will be approached in cavities having a large fraction of surfaces that face the aperture at oblique angles because, in this case, a large fraction of emitted bundles are absorbed before exiting the cavity. When relation (12) is considered with the variance, the result is that, for the emission

method, the overall convergence speed measured by ray-tracing processing time decreases as the number of oblique surfaces increases.

The absorption method should not experience the same slowing in convergence speed. In contrast to the emission method, the bundle density for the absorption method does not change as the cavity geometry becomes more complex because the bundles are emitted from the aperture. Although the variance of the absorption method would be expected to increase as the number of oblique surfaces increases, the increase in variance should be much smaller because the bundle density is constant in this case. When the average number of reflections \bar{r} is examined, one sees that the average number of reflections per bundle is not limited by absorption probability as it is in the emission method because each impact only reduces the statistical weight of the bundle. The average number of reflections is instead limited by the numerical round-off error truncation given in inequality (6). Although \bar{r} for the absorption method may be many times larger than that for the emission method, relation (12) indicates that the expected large reduction in the number of bundles required for convergence, N , allows the absorption method to have an overall convergence speed that is faster than the emission method when applied to cavities with many oblique surfaces.

The third comparison to be made between the two Monte Carlo methods deals with the case of normal emittance. In the laboratory, blackbody cavities are usually positioned behind a limiting aperture of high reflectivity to reduce stray thermal signal originating on the front surface of the blackbody source. For this reason, the normal emittance of the source or the emittance of the source through an aperture located at a finite distance from the source is often needed. To properly model this setup, this aperture surface must be introduced into the analysis. As the aperture is moved further away from the source, the effective source aperture as seen from the walls of the cavity is reduced in size, which in turn decreases the aperture surface area to cavity wall surface area ratio. Thus, when we increase the distance between source and aperture, it has the same effect as increasing the surface area of the cavity. As shown above, this increase in cavity surface area decreases the overall convergence speed of the emission method. A similar problem exists for the emission method if the blackbody source is imaged through a lens or mirror. In this case, the aperture is narrowed to a point at the focal distance of the optics in question, which has the identical effect of creating an effective infinite cavity surface area A_w . Equation (11) then shows that, in this case, an infinite number of bundles is needed to produce a finite bundle density. In other words, as a limiting aperture is brought to an infinitesimal point, the statistical probability of a ray exiting the blackbody source and then hitting the aperture approaches zero.

The absorption method does not suffer the same limitations as the emission method for normal emit-

tance models. Because the bundles are emitted from the aperture, an increase in the distance between aperture and source only changes the angular distribution function of these emitted bundles. Each bundle still contributes information to the measurement of the aperture apparent emissivity according to Eq. (8), and therefore no increase in the number of bundles is required for an accurate solution. In addition, if the blackbody source is imaged through optics, one merely sets the origin of all bundles to a focal point of the optics, and a convergent solution can be found.

One last difference between the two methods is in the information available from each method. In the emission method, each surface emits bundles of a prescribed energy, and so an estimate of the radiative flux at every surface can be calculated when we track the number of bundles emitted and absorbed at that surface. This information can then be used to aid in the thermal design of the blackbody source. In contrast, the absorption method does not readily supply information outside of a description of the emitted spectrum. For this reason, the absorption method is not as widely used in general radiative analysis.

3. Analysis and Results

A. Convergence Analysis

When we examine the differences between the emission and the absorption methods, one item that deserves closer examination is the speed of convergence. However, before a direct comparison between the two methods can be made, compatible convergence criteria are needed. As previous authors have shown,¹² the convergence for the emission Monte Carlo method can be found in terms of the variance of the algorithm output $\sigma_{\epsilon_{app}}^2$. Use of $\sigma_{\epsilon_{app}}^2$ is possible for the emission method because the results of each individual bundle follow a binomial distribution, where each bundle either exits the aperture or is absorbed. The variance of such a zero-one distribution is well known and easily calculated. In the absorption method, however, the variance-based convergence criteria fail. The failure occurs because, in this method, each ray is partially absorbed before exiting the aperture. If the results of a large number of bundles are tracked, it is found that the results follow a multinomial distribution. The variance of such a distribution is extremely difficult to calculate, and so new convergence criteria that are compatible with both methods need to be established.

To do so, we developed new convergence criteria based on a linear least-squares method. In this technique, an intercept for the first least-squares line is chosen. The choice of this first intercept is somewhat arbitrary because Monte Carlo solutions rarely converge quickly. Using this set intercept, we performed a least-squares fit on the first n results of the Monte Carlo algorithm. Using the resulting linear equation, we determined the intercept for the next least-squares line for the next set of n results. The

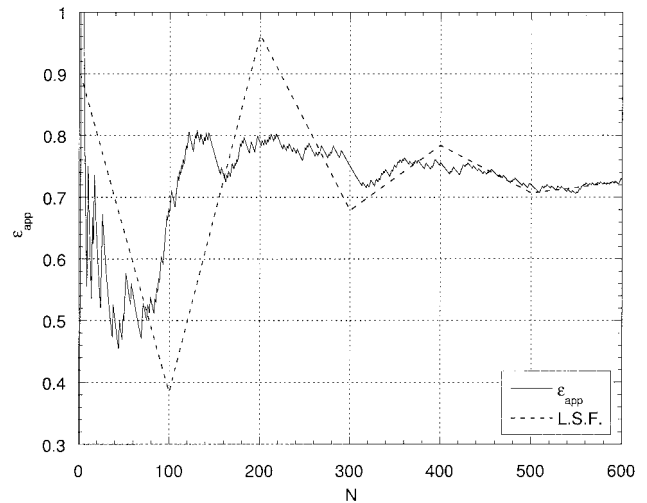


Fig. 2. Plot of apparent emissivity versus N along with the calculated least-squares fit (L.S.F.) lines showing how the estimated slope of the least-squares lines approaches zero as N increases.

least-squares analysis is repeated for each consecutive set of n results, resulting in a continuous series of lines constructed from the output of the Monte Carlo algorithm. An example of this convergence technique is shown graphically in Fig. 2 where the least-squares fit lines are superimposed over the apparent emissivity versus N data. If one looks at the point-wise output of the Monte Carlo algorithm as a function of emitted bundles, one first can see a widely varying function that slowly converges to a solution as the overall number of bundles emitted, N , increases. The series of least-squares lines therefore converge to lines with a slope near zero and having a small variance. The convergence criteria of the Monte Carlo algorithm are thus established by use of these properties.

From a least-squares analysis, the set variance s_{ϵ}^2 about its fit line with estimated slope α^* is found to be

$$s_{\epsilon}^2 = \left(\frac{1}{n-1} \right) \sum_{k=1}^n [(\epsilon_k - \epsilon_0) - \alpha^*(N_k - N_0)]^2. \quad (14)$$

An estimation of the true slope α^* is found from the set data by

$$\alpha^* = \frac{\sum_{k=1}^n (N_k - N_0)(\epsilon_k - \epsilon_0)}{\sum_{k=1}^n (N_k - N_0)^2}, \quad (15)$$

where N_0 and ϵ_0 are the coordinates of the origin of the line determined by the end point of the previous least-squares line. The convergence criteria of the Monte Carlo methods are determined by the statistic

$$t = \frac{\bar{\epsilon}^* - \bar{\epsilon}}{s_{\epsilon}/\sqrt{n}}, \quad (16)$$

where $\bar{\epsilon}^*$ and $\bar{\epsilon}$ are the average estimated and true set results, respectively, and are given by

$$\bar{\epsilon}^* = \frac{1}{n} \sum_{k=1}^n a^*(N_k - N_0) + \epsilon_0, \quad (17)$$

$$\bar{\epsilon} = \frac{1}{n} \sum_{k=1}^n a(N_k - N_0) + \epsilon_0. \quad (18)$$

Simplifying Eq. (16), a statistic following the Student's t distribution,

$$t = \frac{(a^* - a)\bar{N}}{s_\epsilon/\sqrt{n}}, \quad (19)$$

is found, where \bar{N} is the average value of N_k over the set of n points used for the least-squares fit. At large sample sizes ($n > 20$), the normal distribution can be substituted for the Student's t distribution. When we use the normal distribution, the probability of t being less than some value δ is given by

$$\text{Prob}(|t| < \delta) = \text{Prob}\left[\left|\frac{(a^* - a)\bar{N}}{s_\epsilon/\sqrt{n}}\right| < \delta\right] = \text{erf}\left(\frac{\delta}{\sqrt{2}}\right), \quad (20)$$

which can be rewritten as

$$\text{Prob}\left[|(a^* - a)\bar{N}| < \frac{\delta s_\epsilon}{\sqrt{n}}\right] = \text{erf}\left(\frac{\delta}{\sqrt{2}}\right). \quad (21)$$

For convergence, two conditions relating to Eq. (21) must be held. First, the criteria for convergence must be set. Convergence can be said to occur when the difference between the average estimated and average true results is less than a small specified number β :

$$|(a^* - a)\bar{N}| < \beta. \quad (22)$$

The value for β is chosen somewhat arbitrarily in that the needed degree of convergence varies from application to application. However, a general guideline for the choice of β found from numerical experiments is that $10^{-7} < \beta < 10^{-5}$. Once β is set, the following relation for convergence is established:

$$\frac{\delta s_\epsilon}{\sqrt{n}} \leq \beta. \quad (23)$$

When we look at Eq. (21) and inequality (23), the second convergence condition, which determines the value of δ , can be explained. For a given value of β , the probability of the meeting of convergence criteria signaling the true convergence must be high (i.e., the probability of a random-chance nonconvergent result meeting the convergence criteria is low). A high probability means that the right-hand side of Eq. (21) must equal a high percentage (for example, 95%). From this condition, the value of δ can be established by use of standard tables listing the value of the error function (e.g., in the case of 95% probability, $\delta = 1.96$). After both δ and β are fixed, convergence can

be determined when a set of the Monte Carlo algorithm gives a variance s_ϵ^2 , which satisfies inequality (23). However, s_ϵ^2 itself can have a large variance leading to variability in the number of sets required for convergence for a given model analysis. For this reason, a moving average of s_ϵ^2 is used in place of s_ϵ^2 in inequality (23) to reduce the variability in convergence time.

In this convergence analysis, one important assumption was made. The least-squares analysis assumes that, for each point of the set N_k , the variance of ϵ_k about the true value ϵ is identical. This assumption is not strictly held here. A clear violation of this assumption occurs if the complete set of N bundles from a convergent solution is used for the least-squares fit. If many different complete trials are done, it would be found that the result of the first bundle would have a large variance, where the last (and convergent) result would have a small variance. For this reason, one must take care when setting the size of the data sets n used for the least-squares fit. If the set is too large, the results given above will not be valid, and convergence may be overestimated.

B. Example Model Analysis

With compatible convergence criteria established, the convergence properties of the emission and absorption methods can be explored. To illuminate the differences between the two methods, a cylindrical blackbody source of length L and radius R is used to show a simple cavity transitioning to one having a large fraction of surfaces facing the aperture at oblique angles. At a small length-to-radius ratio L/R , the geometry of this cavity is such that a small fraction of the total cavity wall surface area has a low probability of emitted or reflected rays reaching the aperture. At large values of L/R , a large fraction of the total cavity wall surface area has a low probability of emitted or reflected rays reaching the aperture.

The analysis of the cylinder was performed as follows. In both emission and absorption methods, the cavity wall surfaces are assumed to be isothermal, gray, and diffuse. As stated above, the ray-tracing subroutine usually exacts the largest computational cost in Monte Carlo analysis. The computational time for convergence is therefore measured in terms of the number of calls to the ray-tracing subroutine. This measurement is standardized between the two methods by use of an identical ray-tracing subroutine in both computer codes. In addition, both methods use the same combined linear congruential random-number generator¹³ to equalize pseudo-random-number generation and computational cost. To establish consistent convergence criteria between both methods, each will use the least-squares convergence criteria stated above with a set size n of 100 with a 95% probability ($\delta = 1.96$), a β value of 2×10^{-6} , and with the previous ten values of s_ϵ^2 for the moving average of s_ϵ^2 in inequality (23). We determined this value of β by comparison of the least-squares convergence method with the standard

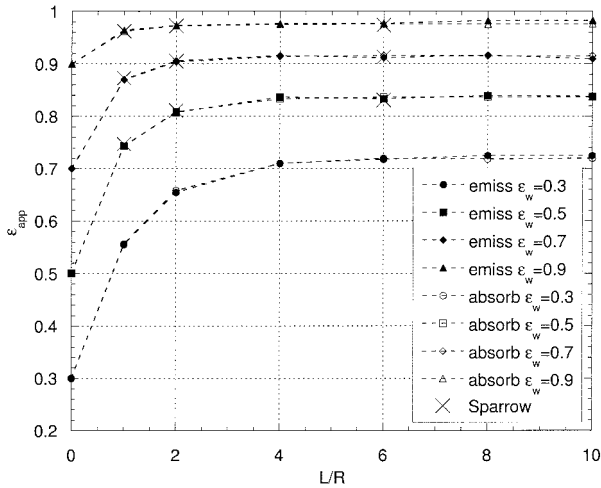


Fig. 3. Plot of the apparent emissivity versus L/R for a right cylinder for both emission and absorption methods showing agreement with previous results (see Sparrow *et al.*¹) at multiple surface emissivities and a range of values of L/R .

variance convergence method using a cylinder with a L/R value of 1 and $\epsilon_w = 0.5$.

The algorithms used for the emission and absorption method follow that of previous authors.^{8,14} For the emission method algorithm, the location on the cavity surface of each emitted bundle is found according to the distribution functions derived from Eqs. (9) and (10). The direction of the bundle is determined by a diffuse, gray reflection distribution function.¹⁴ The bundles are then traced to the next surface where we determined absorption or reflection by comparing a pseudo randomly generated number to the reflectivity of the surface. The bundles then continue to be diffusely reflected or absorbed until absorption occurs or the bundle exits the cavity. If the bundle exits the aperture, it is added to the running tally. For the absorption method algorithm, the origin of the bundle on the aperture surface is determined by a distribution function. The bundle is then diffusely reflected about the cavity until either the bundle exits the cavity or the number of reflections reaches the reflection limit m^* . At each reflection, the weight of the bundle is tallied according to Eq. (8).

We perform the analysis of convergence speed by first looking at the output of the two methods and comparing them with an analytical solution. Figure 3 shows the comparison and indicates that both methods result in an accurate solution over a wide range of L/R and surface emissivity, as expected. In convergence to these solutions, the average number of calls to the ray-tracing subroutine per traced bundle, the number of bundles required for convergence, and the total number of ray-tracing subroutine calls are recorded. Figure 4 is a plot of the average number of calls to the ray-tracing subroutine per traced bundle \bar{r} as a function of L/R . For the emission method, it can be seen that, at large values of L/R , where many of the rays are absorbed by the cavity

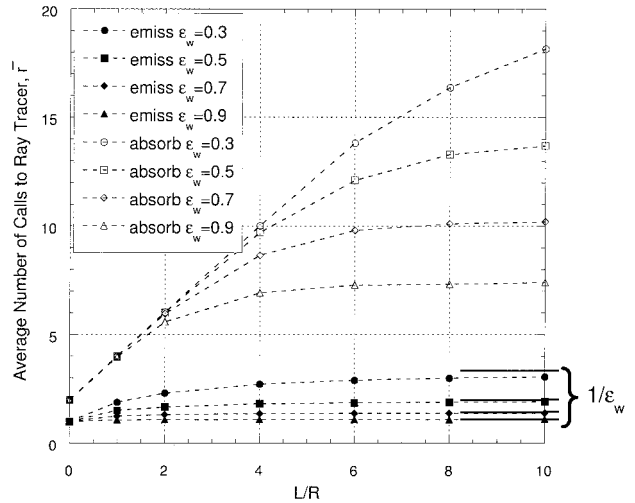


Fig. 4. Average number of calls to the ray-tracing subroutine is plotted versus L/R for both the emission and the absorption methods for various values of cavity wall emissivity ϵ_w . The average number of ray traces per bundle for the absorption method is much larger than for the emission method at all surface emissivities and values of L/R . The emission method approaches the theoretical $1/(1 - \rho_w) = 1/\epsilon_w$ limit at large L/R .

walls, \bar{r} approaches $1/(1 - \rho_w) = 1/\epsilon_w$, as predicted. The value of \bar{r} for the absorption method is up to seven times larger than that for the emission method for a value of Er in inequality (6) of 1×10^{-12} . To determine the validity of our choice of Er , the apparent aperture emissivity is plotted as a function of m^* for several values of surface emissivity and a L/R value of 10 in Fig. 5. Figure 5 shows that our choice of Er results in a m^* value that is much higher than what is required for an accurate solution. If a larger value of Er is used resulting in a smaller m^* , the average number of ray-tracing subroutine calls per bundle will decrease; therefore the absorption

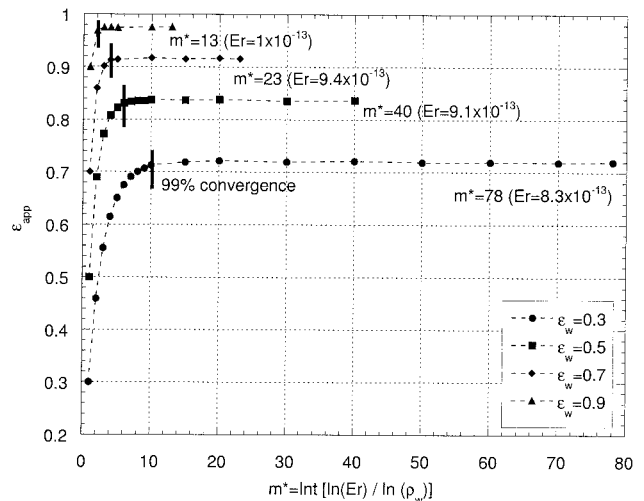


Fig. 5. Apparent emissivity is plotted versus the truncation limit m^* for the absorption method showing that the limit used in this paper is much larger than what is needed for accurate solution convergence.

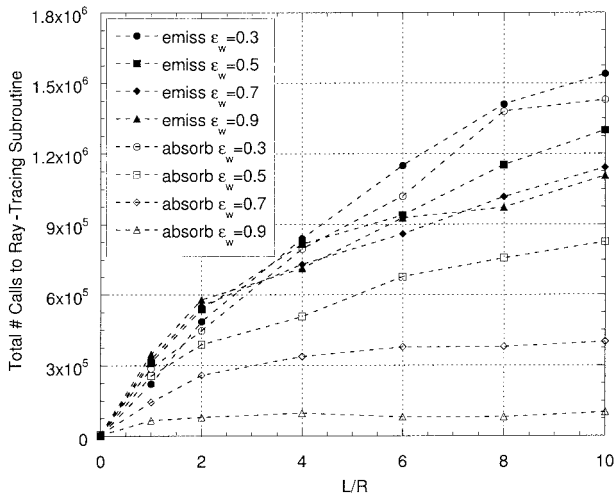


Fig. 6. Total number of calls to the ray-tracing subroutine is plotted versus L/R for the emission and absorption methods. For complex geometry (i.e., large values of L/R), the absorption method converges more rapidly than the emission method.

method will converge faster than is shown in this example. For this reason, the convergence speed data shown here represents a worse-case situation and could be improved by a better choice of E_r leading to a smaller reflection truncation limit m^* . This difference in average subroutine calls between the two methods is indicative of the key computational difference between the two methods. In the emission method, the bundle is either completely absorbed at each surface, eliminating any subsequent ray tracing, or it is completely reflected, requiring further traces. In contrast, each bundle in the absorption method is reduced in weight upon each impact, and therefore the ray tracing ends only if the ray exits the aperture or if the number of reflections meets the reflection truncation limit m^* .

Although the average number of subroutine calls per traced bundle for the absorption method is much larger than that for the emission method, the overall total number of calls to the ray-tracing subroutine for convergence, and hence convergence speed, of the absorption method is much smaller than that for the emission method. The overall convergence speed, measured in the total number of calls to the ray-tracing subroutine, is plotted in Fig. 6. In Fig. 6, as L/R is increased the difference in convergence speed between the two methods increases dramatically, especially for high values of cavity surface emissivity. At the largest L/R and largest surface emissivity shown here, the absorption method converges an order-of-magnitude faster than the emission method. This apparent disagreement between the large average number of subroutine calls per bundle and the small overall convergence speed can be explained when we look at the number of least-squares sets needed for convergence, which is shown in Fig. 7. As the geometry is made to have more oblique surfaces with an increase in L/R , the number of sets required for convergence for the absorption method remains

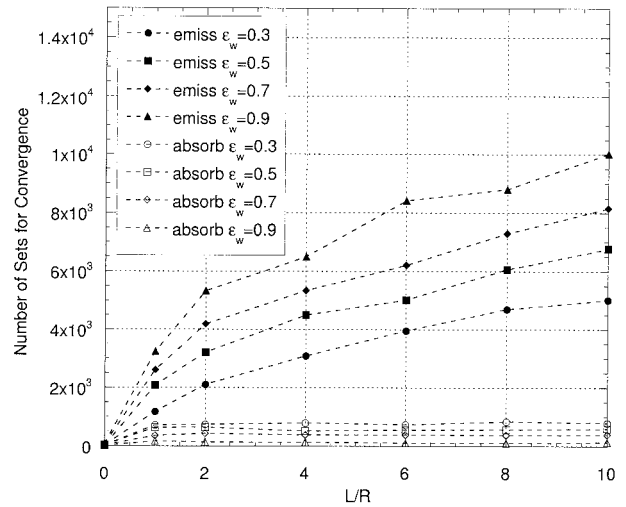


Fig. 7. Plots of the number of least-squares sets required for convergence versus L/R for the emission and absorption methods showing that the advantage in speed of convergence of the absorption method is caused by the reduced number of least-squares sets required for a convergent solution.

constant, but increases monotonically for the emission method. As explained above, the emission method is dependent on a cavity bundle density that decreases as the geometry is made larger. This decrease in surface bundle density results in a larger set variance requiring a larger number of sets for convergence. The absorption method, in contrast, has a constant bundle density over the aperture surface, which is independent of changes to the cavity geometry. The set variances of the absorption method do not change, and so this method does not require an increase in the number of sets required for convergence as the cavity is made to have more oblique surfaces.

For sources with nonisothermal wall properties, results with the same general properties as those discussed here are expected. Experimental blackbody cavities are designed to keep temperature gradients to a minimum. It is therefore expected that, with respect to the behavior of set variance of the two methods, the effects of a change in the cavity geometry will dominate over the effects of small variations in cavity wall temperature. In addition, variable surface temperatures mean that the emission method requires more complicated distribution functions to determine the origin of the bundles emitted from the surfaces.¹⁴ The absorption method requires only a weighting term dependent on the local temperature⁷ to be included in Eq. (8) and therefore is easier to implement than the emission method for nonisothermal cavities.

4. Summary and Conclusions

We have presented two methods for the application of the Monte Carlo technique to the problem of finding blackbody cavity apparent emissivity. The fundamental differences between the two methods were

explained from a brief outline of the analytical basis of the two methods. In the emission Monte Carlo method, each surface of the blackbody cavity emits bundles of a prescribed energy that are completely absorbed or completely reflected by each consecutive surface according to distribution functions derived from surface properties. In the absorption Monte Carlo method, bundles are traced from the aperture and are statistically weakened at each surface interaction until their statistical weight is reduced to a value below the accuracy limit of the computer system involved.

The two methods were compared on the basis of ease of implementation. In the development of the Monte Carlo algorithm, the absorption method required fewer and simpler distribution function calculations than the emission method. The absorption method was also preferred to the emission method when applied to the case of normal emittance or in use of optics. However, the emission Monte Carlo method is advantageous in that it provides local heat flux information that can be useful in the design of experimental sources.

New compatible least-squares fit convergence criteria for the comparison of convergence speed of both methods were developed. Using this convergence criteria, we applied both methods to a right cylinder of length L and radius R . The values of L/R and ϵ_w were varied to quantify the convergence behavior of the two methods as the cylindrical cavity was lengthened and the surface emissivity was changed. It was found that, although the average number of calls to the ray-tracing subroutine was much larger for the absorption method than for the emission method for larger values of L/R , the number of least-squares sets required for convergence was much smaller for the absorption method than for the emission method. This smaller number of required least-squares sets resulted in the absorption method having a much faster overall convergence speed, which was explained in terms of the dependency of the variance of each least-squares set on the surface bundle density.

From these results it can be concluded that the absorption method is preferred over the emission method in the application of the Monte Carlo technique to the calculation of blackbody aperture appar-

ent emissivity for cavities with a large number of surfaces that face the aperture at oblique angles.

The authors acknowledge the National Science Foundation (NSF) for the support of this study through grant CTS-95-27983. Any opinions, findings, conclusions, or recommendations expressed in this publication are those of the authors and do not necessarily reflect the views of the NSF.

References

1. E. M. Sparrow, R. P. Heinisch, and N. Shamsundar, "Apparent hemispherical emittance of baffled cylindrical cavities," *J. Heat Transfer* **96**, 112–114 (1974).
2. R. P. Heinisch, E. M. Sparrow, and N. Shamsundar, "Radiant emission from baffled conical cavities," *J. Opt. Soc. Am.* **63**, 152–158 (1973).
3. N. Shamsundar, E. M. Sparrow, and R. P. Heinisch, "Monte Carlo radiation solutions—effect of energy partitioning and number of rays," *Int. J. Heat Mass Transfer* **16**, 690–694 (1973).
4. R. C. Corlett, "Direct Monte Carlo calculation of radiative heat transfer in vacuum," *J. Heat Transfer* **88**, 376–382 (1966).
5. A. Ono, "Calculation of the directional emissivities of cavities by the Monte Carlo method," *J. Opt. Soc. Am.* **70**, 547–554 (1980).
6. J. Ishii, M. Kobayashi, and F. Sakuma, "Effective emissivities of black-body cavities with grooved cylinders," *Metrologia* **35**, 175–180 (1998).
7. A. V. Prokhorov, "Monte Carlo simulation of the radiative heat transfer from a blackbody to a cryogenic radiometer," in *Optical Radiation Measurements III*, J. M. Palmer, ed., Proc. SPIE **2815**, 160–168 (1996).
8. V. I. Sapritsky and A. V. Prokhorov, "Calculation of the effective emissivities of specular-diffuse cavities by the Monte Carlo method," *Metrologia* **29**, 9–14 (1992).
9. V. Sapritsky and A. Prokhorov, "Spectral effective emissivities of nonisothermal cavities calculated by the Monte Carlo method," *Appl. Opt.* **34**, 5645–5652 (1995).
10. M. J. Ballico, "Modelling of the effective emissivity of a graphite tube black body," *Metrologia* **32**, 259–265 (1996).
11. Y. Ohwada, "Numerical calculation of multiple reflections in diffuse cavities," *J. Opt. Soc. Am.* **71**, 106–111 (1981).
12. W. J. Minkowycz, *Handbook of Numerical Heat Transfer* (Wiley-Interscience, New York, 1988).
13. P. L'Ecuyer, "Efficient and portable combined random number generators," *Commun. ACM* **31**, 742–774 (1988).
14. R. Siegel and J. R. Howell, *Thermal Radiation Heat Transfer*, 3rd ed. (Hemisphere, Washington, D.C., 1992).